Phase II Study of KW-0761 for Relapsed ATL, 第９回日本臨床腫瘍学会学術集解, 2011

3. 塚崎邦弘： ATL に対する臨床試験の現状と患者参加促進. 第 73 回日本血液学会学術集会, 2011
4. Nagai H, Tsukasaki K, et al：第 73 回日本血液学会学術集会: Phase I Study of Forodesine in Patients with Relapsed or Refractory T/NK-Cell Malignancies,2011
5. Taniguchi H, , Tsukasaki K, et al：Outcome of adult T-cell leukemia-lymphoma(ATL)after salvage therapy, 第 73 回日本血液学会学術集会, 2011
6. Uchimaru K, Tsukasaki K, et al： Nation-wide survey of the management of adult T-cell leukemia and HTLV-1 carrier, 第73回日本血液学会学術集会, 2011.
7. Yamamoto K, Tsukasaki K, et al. : Plenary Session. Phase II/III trial of RCHOP-21 vs. RCHOP-14 in untreated advanced indolent B-cell lymphoma : JCOG0203, 第 73 回日本血液学会学術集会, 2011
8. Makiyama J, Tsukasaki K, et al : Methotrexate-associated lymphoproliferative disorders in patients with rteumatoid arthritis, 第 73 回日本血液学会学術集会, 2011
9. Maruyama D, Tsukasaki K, et al : Phase I study of forodesine(BCX1777),an oral purine nucleoside phosphorylase inhibitor in patients with relapsed or refractory T/NK-cell malignancies, T-CELL LYMPHOMA FORUM, 2011.
10. Tsukasaki K : Pathogenesis of Adult T cell Leukemia-Lymphoma. XI Simpósio Internacional sobre HTLV no Brasil, 2011.
11. Tsukasaki K : International consensus on the management of ATL. XI Simpósio Internacional sobre HTLV no Brasil, 2011.
12. Tsukasaki K : Clinical Trials for the Treatment of adult T-cell leukemia/lymphoma (ATLL) by the Japan Clinical Oncology Group (JCOG). XI Simpósio Internacional sobre HTLV no Brasil, 2011.
13. Utsunomiya A, Tsukasaki K, et al : Promising Results of an Anti-CCR4 Antibody, KW-0761, for Relapsed Adult T-Cell Leukemia-Lymphoma(ATL). 15th International Conference on Human Retrovirology HTLV and Related Viruses, 2011
14. K. Tobinai, , Tsukasaki K, et al: Promising Results of an Anti-CCR4 Antibody, KW-0761, for Relapsed Adult T-Cell Leukemia-Lymphoma(ATL), 11th International Conference on Malignant Lymphoma, 2011.
15. Katsuya H, Tsukasaki K, et al: A Prognostic Index for Acute and Lymphoma Type Adult T-Cell Leukemia/Lymphoma. 53rd ASH Annual Meeting, 2011.
16. Fukushima T, Tsukasaki K, et al. Characterization of Long Term Survivors and a Predictive Model for Aggressive Adult T-Cell Leukemia-Lymphoma(ATL):An Ancillary Study by the Japan Clinical Oncology Group,JCOG0902A. 4th Annual T-cell Lymphoma Forum, 2012.
17. Fukushima T, Tsukasaki K, et al. Characterization of Long Term Survivors and a Predictive Model for Aggressive Adult T-Cell Leukemia-Lymphoma(ATL):An Ancillary Study by the Japan Clinical Oncology Group,JCOG0902A. 53rd ASH Annual Meeting, 2011.
18. Tsukasaki K, et al. JCOG studies for ATL. 4th Annual T-cell Lymphoma Forum, 2012.

G. 知的所有権の出願・取得状況

1. 特許取得　なし

III. 研究成果の刊行に関する一覧表

雑誌

発表者氏名	論文タイトル名	発表誌名	巻号	ページ	出版年
Yamagishi M, Nakano K, Miyake A, Yamochi T, Kagami Y, Tsutsumi A, Matsuda Y, Sato-Otsubo A, Muto S, Utsunomiya A, Yamaguchi K, Uchimaru K, Ogawa S, Watanabe T	Polycomb-mediated loss of miR-31 activates NIK-dependent NF-kB pathway in adult T-cell leukemia and other cancers	***Cancer Cell***	21(1)	121-135	2012
Umino A, Tsukasaki K, et al.	Clonal evolution of adult T-cell leukemia/lymphoma takes place in lymph node.	***Blood***	117	5473-5478	2011
Watanabe T	Current status of HTLV-1 infection	***Int J Hematol***	94(5)	430-434	2011
渡邉俊樹	特集 感染に由来するヒトの腫瘍—その現状と対策:「成人T細胞白血病ウイルスと白血病/リンパ腫」	*臨床と微生物*	38（3）	241-248	2011
渡邉俊樹	特集 分子病態からみた血液疾患診療の進歩:「ATLの分子病態と治療の新展開」	*血液内科*	62（4）	455-462	2011
山岸誠、渡邉俊樹	成人T細胞白血病から明らかになったクロストーク異常とがん	*ライフサイエンス新着論文レビュー* http://first.lifesciencedb.jp/archives/4367	52(10)	27-35	2012

IV. 研究成果の刊行物・別刷

Cancer Cell
Article

Polycomb-Mediated Loss of miR-31 Activates NIK-Dependent NF-κB Pathway in Adult T Cell Leukemia and Other Cancers

Makoto Yamagishi,[1,3] Kazumi Nakano,[1] Ariko Miyake,[1] Tadanori Yamochi,[1] Yayoi Kagami,[1] Akihisa Tsutsumi,[1] Yuka Matsuda,[1] Aiko Sato-Otsubo,[4] Satsuki Muto,[1,4] Atae Utsunomiya,[5] Kazunari Yamaguchi,[6] Kaoru Uchimaru,[2] Seishi Ogawa,[4] and Toshiki Watanabe[1,*]
[1]Graduate School of Frontier Sciences
[2]Institute of Medical Science
The University of Tokyo, Tokyo, 108-8639, Japan
[3]Japan Foundation for AIDS Prevention, Tokyo, 101-0061, Japan
[4]Cancer Genomics Project, Graduate School of Medicine, The University of Tokyo, Tokyo, 113-8655, Japan
[5]Department of Haematology, Imamura Hospital, Bun-in, Kagoshima, 890-0064, Japan
[6]Department of Safety Research on Blood and Biologics, NIID, Tokyo, 208-0611, Japan
*Correspondence: tnabe@ims.u-tokyo.ac.jp
DOI 10.1016/j.ccr.2011.12.015

SUMMARY

Constitutive NF-κB activation has causative roles in adult T cell leukemia (ATL) caused by HTLV-1 and other cancers. Here, we report a pathway involving Polycomb-mediated miRNA silencing and NF-κB activation. We determine the miRNA signatures and reveal miR-31 loss in primary ATL cells. MiR-31 negatively regulates the noncanonical NF-κB pathway by targeting NF-κB inducing kinase (NIK). Loss of miR-31 therefore triggers oncogenic signaling. In ATL cells, miR-31 level is epigenetically regulated, and aberrant upregulation of Polycomb proteins contribute to miR-31 downregulation in an epigenetic fashion, leading to activation of NF-κB and apoptosis resistance. Furthermore, this emerging circuit operates in other cancers and receptor-initiated NF-κB cascade. Our findings provide a perspective involving the epigenetic program, inflammatory responses, and oncogenic signaling.

INTRODUCTION

Adult T cell leukemia (ATL) is an aggressive T cell neoplasm with very poor prognosis (Yamaguchi and Watanabe, 2002). Human T cell leukemia virus type I (HTLV-I) is recognized as an etiological factor in T cell malignancy. Although mounting molecular evidence has contributed to our ability to cure several cancers and other diseases, the genetic background of ATL leukemogenesis is not yet fully understood. Thus, it is an urgent request to clarify the molecular mechanism of ATL development.

Constitutive activation of nuclear factor-κB (NF-κB) is observed in the ATL cell lines and primary isolated tumor cells from ATL patients, although the viral oncoprotein Tax, a powerful activator of NF-κB, is not expressed in these malignant cells (Hironaka et al., 2004; Watanabe et al., 2005). NF-κB activation aberrantly contributes to cell propagation and anti-apoptotic responses in ATL and other cancers (Prasad et al., 2010). In our previous study, inhibition of NF-κB activity with a specific inhibitor, DHMEQ, drastically impaired the levels of ATL cell growth and resistance to apoptosis (Watanabe et al., 2005), suggesting that the molecular background of aberrant NF-κB activation may give us potential therapeutic targets. A recent report provided a new readout that NF-κB-inducing kinase (NIK) has a causal role in tumor progression and the aggressive phenotypes of various cancers, including ATL (Saitoh et al., 2008). NIK plays a pivotal role in the noncanonical (alternative) NF-κB pathway as a crucial kinase in receptor-initiating signaling, including signaling from CD40, LTBR, and BAFFR.

Significance

Here, we propose a molecular perspective of the onset of oncogenic signaling. NIK overexpression is a major driving force for constitutive NF-κB activation in various types of cancers. Using ATL cells as a model of NF-κB-addiction, we identified miR-31 as a suppressor of NIK that is completely silenced in ATL cells. Furthermore, an oncogenic function of a subset of Polycomb is implicated in NF-κB signaling via miRNA regulation. This study introduces a fundamental link between the Polycomb-mediated epigenetic regulation and the NF-κB signaling, allowing us to attribute the constitutive activation of NF-κB to epigenetic reprogramming.

Several studies have recently implicated another functional significance of NIK protein in epithelial cell proliferation, inflammatory response, and oncogenic signaling (for review, see Thu and Richmond, 2010). Although the expression level of NIK is strictly maintained by proteasomal degradation in normal cells (Liao et al., 2004), increased level of NIK transcript are observed in some cancers, causing inappropriate accumulation of NIK protein without stimuli (Annunziata et al., 2007; Saitoh et al., 2008). Overexpression of NIK leads to aberrant phenotypes in several cell types; however, little is known about the abnormal accumulation of NIK in malignant cells.

Recent advances have led to deeper understanding of a new aspect of posttranscriptional gene regulation, i.e., regulation by a class of noncoding RNAs. MicroRNAs (miRNAs) are functional RNAs with 18–25 nt in length that contribute to a class of cellular functions by negatively controlling targeted gene expression via base-pairing to 3′ untranslated region (3′ UTR). A single miRNA regulates the expression of multiple genes, and the functions of miRNAs therefore need to be orchestrated for cellular homeostasis (Ventura and Jacks, 2009). In the context of cancer pathology, many studies have provided evidences that miRNAs can act as either oncogenes or tumor suppressors. Although the relationship between miRNA deregulation and oncogenes has been clarified in several cancer cells, there has been no integrated analysis of gene expression in ATL. Since miRNAs have important functions in living cells, miRNA expression needs to be tightly regulated. Our knowledge about the regulatory mechanisms of miRNA expression is very inadequate because research effort has focused mainly on the role of miRNAs, which remains one of the most intriguing questions. miRNA regulation involves multiple steps. miRNA maturation has been identified as an important step, and its deregulation leads to progression and development of cancer (Davis et al., 2008; Trabucchi et al., 2009). Genetic deletion in cancer cells has also been reported to account for specific miRNA defect (Varambally et al., 2008). In addition, miRNA expression seems to be epigenetically programmed. DNA methylation and histone modification are strong candidates for miRNA regulation and their abnormalities, therefore, have causal roles in cancer initiation, development, and progression. In particular, Polycomb group proteins have central functions in cellular development and regeneration by controlling histone methylation, especially at histone H3 Lys27 (H3K27), which induces chromatin compaction (Simon and Kingston, 2009). Recent studies have revealed that the amount of Polycomb family is closely associated with cancer phenotypes and malignancy in breast cancer, prostate cancer, and other neoplasms (Sparmann and van Lohuizen, 2006). However, the substantial status of Polycomb family and their epigenetic impact in ATL cells have not been documented. Furthermore, the general roles of Polycomb proteins in miRNA regulation are mostly unknown. As described above, since miRNAs are multifunctional molecules in gene regulation, it is of pivotal importance to clarify the miRNAs functions and their regulatory circuit in order to formulate therapeutic strategies.

In the present study, we first performed global miRNA and mRNA profilings of the ATL cells derived from patients to precisely define the significance of miRNA expressions and functions.

RESULTS

miRNA Expression Signature in Primary ATL Cells

To characterize the miRNA expression signature in the primary ATL cells, we first performed an miRNA expression microarray analysis. For results with physiological significance, we used total RNA prepared from clinical ATL samples (n = 40, Table S1 available online) and control CD4+ T cells from healthy donors (n = 22) aged 50–70 years. A strict threshold ($p < 1 \times 10^{-5}$) and two-dimensional hierarchical clustering analysis revealed 61 miRNAs that showed significantly altered levels of expression in ATL cells compared with those of control CD4+ T cells (Figure 1A). It is noteworthy that 59 miRNAs out of 61 (96.7%) showed decreased expression in the primary ATL cells. Among them, we identified miR-31 as one of the most profoundly repressed miRNAs in all ATL individuals (fold change, 0.00403; Figure 1B). miR-31 was recently reported as a tumor suppressor and/or metastasis-associated miRNA in metastatic breast cancer. However, the biological functions of miR-31 in lymphocytes have not been studied. We therefore focused on the biological significance and regulatory mechanisms of miR-31 expression in T cells as well as in solid cancers.

miR-31 Negatively Regulates NF-κB Signaling via NIK Expression

To study the functional significance of miR-31 loss, we attempted to identify the target genes of miR-31 using four computational algorithms. We also performed gene expression microarray analysis of the primary ATL cells (n = 52, Table S1) and normal CD4+ T cells (n = 21) in order to detect aberrations in gene expression. Selected putative target genes are known to be involved in cell-cycle regulation and T cell development (Table S2). To experimentally identify the target genes, we performed reporter-based screens as described below. Luciferase-3′ UTR reporter assays demonstrated a remarkable negative effect against upstream gene expression by the *MAP3K14* 3′ UTR sequence (Figure S1B), which is consistent with an initial cloning report (Malinin et al., 1997). MAP3K14, also known as NIK, has a central role in noncanonical NF-κB signaling by phosphorylation of IKKα. A previous report (Saitoh et al., 2008) and the present results (Table S2) show that NIK is overexpressed in ATL cells, leading to constitutive NF-κB activation. As shown in Figure 2A, treatment with a miR-31 inhibitor increased *NIK* 3′ UTR reporter activity, suggesting the involvement of endogenous miR-31 in NIK downregulation. A computational search predicted one site each of miR-31 and miR-31 antisense (miR-31*) binding sites in the *NIK* 3′ UTR (Figure 2B). To identify the regulatory sequence in 3′ UTR of *NIK*, we established additional two reporters with mutated sequence in each potential seed region (Figure 2C; Figure S1C). Mutant 1, which contains mutated sequence in the miR-31 seed region, partially canceled the negative effect of endogenous miR-31 (Figure S1D) and prevented the effect of Anti-miR-31 treatment (Figure 2D). On the contrary, our results suggest that miR-31* does not participate in NIK regulation. miR-31-mediated reporter regulation was also observed in T cell lines (Figure S1E). To confirm the results, we repeated the experiment to examine whether miR-31 could inhibit NIK expression through seed sequence. We made expression plasmid vectors carrying NIK, NIK-3′

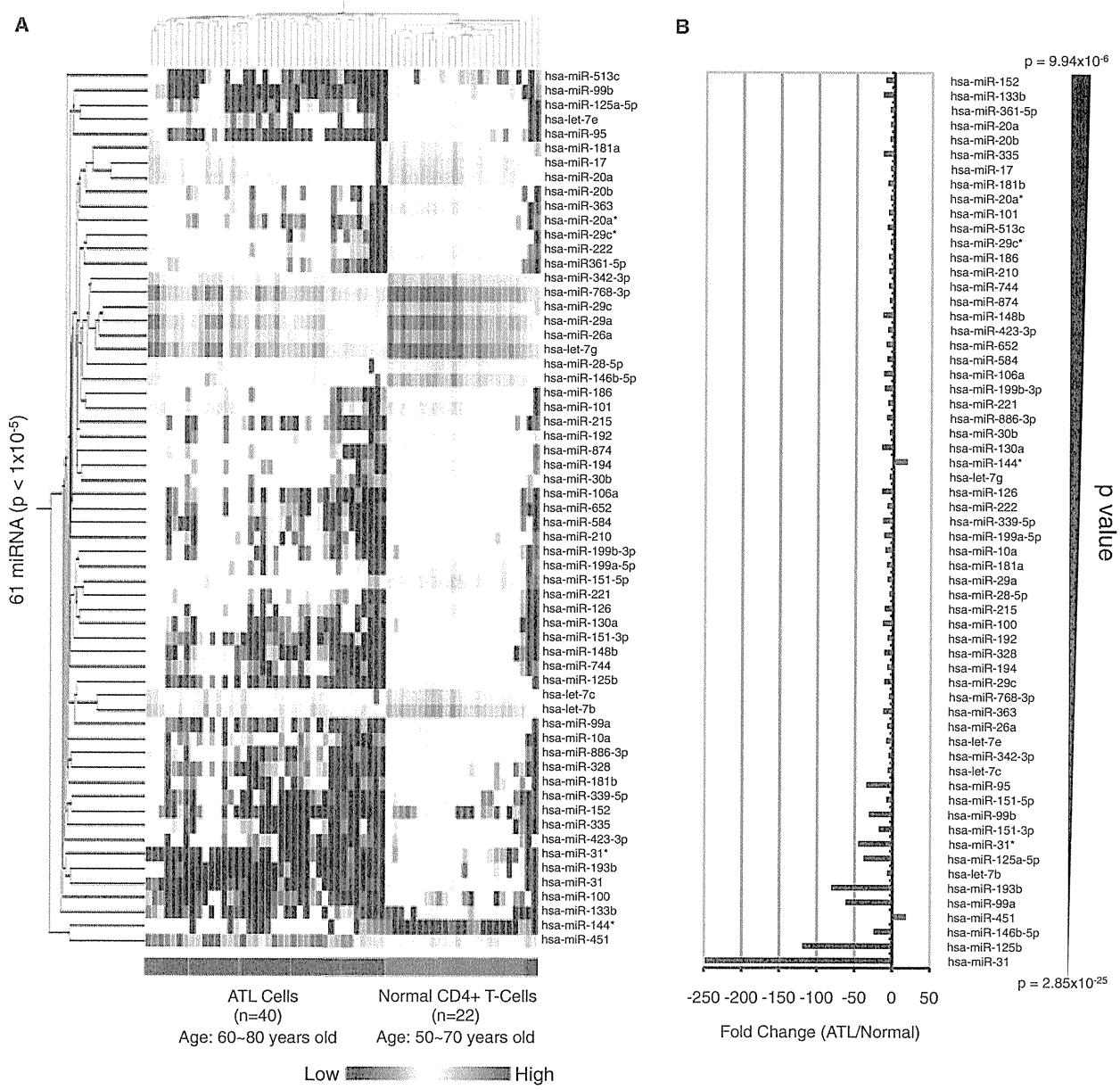

Figure 1. Global Profiling of Cellular miRNA on Primary ATL Cells

(A) Two-dimensional hierarchical clustering analysis and Pearson correlation as similarity measure on the miRNAs expressed at significantly different levels between the ATL (n = 40) and the control (n = 22) groups. Sixty-one miRNAs were identified ($p < 1 \times 10^{-5}$) and by filtering on more than 5-fold changes. A vertical branch shows the expression pattern of the selected miRNAs in each individual.

(B) Fold changes in the 61 miRNAs between ATL and Normal ($p < 10^{-5}$, fold change >5-fold). Selected miRNAs are arranged according to p values. See also Table S1.

UTRWT, or NIK-3′ UTRMu1 and tested their expressions in 293T cells. Results demonstrated that expression of NIK-3′ UTRWT was inhibited by simultaneous introduction of miR-31 (Figure 2E). miR-31 inhibition inversely rescued the NIK level, revealing that the cellular miR-31 level negatively affected that of the NIK protein through its 3′ UTR sequence. These lines of evidence collectively demonstrated that miR-31 recognizes and regulates *NIK* mRNA through specific binding to its 3′ UTR.

Transient introduction of the miR-31 precursor in TL-Om1 cells, which were established from an ATL patient, resulted in downregulation of NIK at the mRNA and protein levels, associated with downregulation of the phospho-IKKα/β level and NF-κB activity (Figures S1F and S1G). In contrast, miR-31 inhibition resulted in accumulation of NIK mRNA and protein in HeLa cells (Figure 2F). Manipulation of the miR-31 level clearly indicated that the miR-31 level negatively correlates with cellular

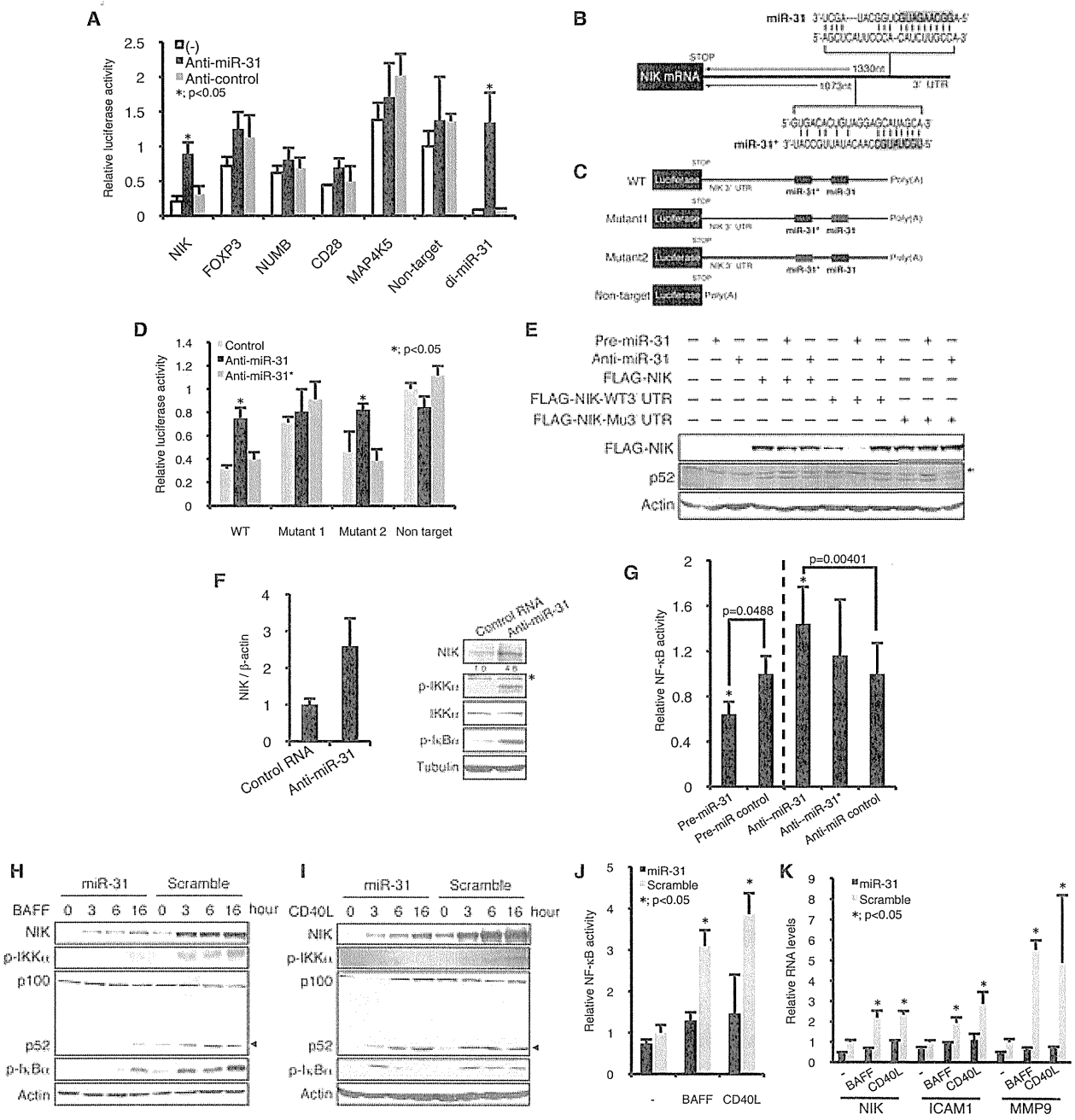

Figure 2. miR-31 Is a Negative Regulator of NF-κB Pathway by Inhibiting NIK Expression

(A) Reporter-based miR-31's target gene screening. A series of 3′ UTR-luciferase reporters was transfected in HeLa cells together with or without miR-31 specific inhibitory RNA (Anti-miR-31) or control RNA (Anti-control). Relative values of Dual-luciferase assay are presented. "Non-target" represents reporter without any 3′ UTR. "di-miR-31" reporter contains two perfect match sequences. The data are presented as mean ± SD of three independent experiments.

(B) Schematic of miR-31 target sites in the *NIK* 3′ UTR.

(C) Mutation-induced reporters. Red box stands for mutated target region (see Figure S1C).

(D) miR-31 negatively regulates *NIK* 3′ UTR analyzed by reporter assay (n = 4, mean ± SD). Luciferase activities of reporter series were tested in a presence or absence of miR-31 inhibitor.

(E) FLAG-tagged NIK protein is negatively regulated through its 3′ UTR and miR-31 binding. Plasmid vectors and miR-31 precursor or miR-31 inhibitor are cotransfected in 293T cells. Western blots showed levels of NIK and endogenous p52. Asterisk indicates nonspecific bands.

(F) NIK mRNA (left) and protein (right) levels in HeLa cells measured by quantitative RT-PCR (n = 3, mean ± SD) and western blotting, respectively. Treatment of miR-31 inhibitor resulted in NIK accumulation. Result of densitometry is shown in the bottom panel. Asterisk indicates nonspecific bands.

(G) Cellular NF-κB activity in HeLa cells (n = 5, mean ± SD) in a presence or absence of miR-31 precursor or inhibitor.

NF-κB activity (Figure 2G). Furthermore, enforced miR-31 expression in B cells attenuated both BAFF and CD40L-mediated NIK accumulation and the subsequent NF-κB signaling (Figures 2H–2K). Consistent with previous reports (Ramakrishnan et al., 2004; Zarnegar et al., 2008b), we also found decreased levels of IκBα phosphorylation. On the other hand, TNF-α-triggered canonical NF-κB activation was not affected by miR-31 in Jurkat cells (Figures S1H–S1K). These results collectively show that miR-31 inhibits the basal and receptor-initiated activities of noncanonical NF-κB pathway. With genetic evidence and an experimental approach, we further demonstrated that the function of miR-31 is well conserved among several classes of species (Figures S1L–S1O). Taking together all these results, miR-31, which is almost completely absent in primary ATL cells, appears to play a critical role in negative regulation of the NF-κB pathway by manipulating the expression of NIK.

miR-31 Suppresses ATL Cell Growth and Promotes Apoptosis by Inhibiting NF-κB

Although it was documented that abnormal NIK accumulation in ATL cells acts as a constitutive activator of the NF-κB pathway, the mechanism underlying overproduction of NIK remains to be elucidated. The results described in the previous section indicated that the amount of miR-31 is linked to the level of NIK, and we therefore speculated that downregulation of miR-31 expression is at least partially responsible for the constitutive activation of NF-κB in ATL cells. Quantitative RT-PCR revealed that *NIK* mRNA levels were negatively correlated with miR-31 levels in primary ATL cell samples (Figure 3A). To investigate the functional roles of NIK and miR-31, we established TL-Om1 cells stably expressing the miR-31 or NIK specific shRNA (shNIK) by retroviral vectors. RT-PCR and western blots showed that expression of miR-31 or shNIK reduced NIK at mRNA and protein levels as well as the levels of phospho-IKKα/β, p52, and IκBα (Figures 3B and 3C). Decreased levels of nuclear RelA and RelB are considered to represent repressed activities of the canonical and noncanonical NF-κB pathways, respectively (Figure 3D). EMSA and NF-κB reporter assays also revealed the repressive function of miR-31 and shNIK on the NF-κB activity (Figures 3E and 3F; Figures S2A, S2B, S5B, and S5C). Re-expression of NIK led to NF-κB activation that was inhibited by miR-31, suggesting a reciprocal relationship between the level of miR-31 and that of NIK.

We and others previously showed that constitutive NF-κB activation is a strong driver of ATL proliferation and prosurvival properties. Here, we examined the effects of miR-31 loss on ATL cell growth. We found that TL-Om1 cells expressing miR-31 or shNIK showed a significant attenuation of cell proliferation compared with control cells. In addition, serum starvation experiments showed greater sensitivity to induced cell death in NIK-repressed cells (Figure 3G). miR-31 expression showed the same phenotypic results in other ATL-derived cell lines (Figures S2C, S2D, and S5E). Jurkat cells do not have significant basal activity of NF-κB, and showed no significant difference in cell growth with or without induced expression of miR-31 (Figure S2E).

Next, we hypothesized that miR-31-mediated NF-κB modulation may affect cellular apoptosis, because numerous studies have demonstrated that NF-κB activation is a strong antiapoptotic factor in ATL and other cancer cells. We found that repression of NIK by miR-31 or shNIK resulted in downregulation of a subset of genes involved in resistance to apoptosis such as BCL-XL, XIAP, and FLIP (Figure 3H), suggesting that miR-31 has a role in proapoptosis through inhibition of NF-κB activity. To assess the biological function of miR-31 in apoptosis signals, we utilized a lentivirus gene transfer system for cell lines and freshly isolated tumor cells. The lentivirus vector is competent to infect nondividing cells and the infected cells can be monitored by the fluorescence of Venus. We found that lentivirus-mediated miR-31 expression promoted basal and Fas-directed apoptosis in TL-Om1 cells (Figure 3I). Venus-negative population showed no significant changes, demonstrating the specificity of miR-31 activity. To confirm the relationship among miR-31, NIK, and NF-κB signaling, we also prepared another retroviral vector encoding NIK without its 3′ UTR sequence. As results, re-expression of NIK reversed the miR-31-mediated apoptosis. In addition, miR-31 expression led to caspase 3 activation (Figure 3J). Collectively, these findings indicate that miR-31 mediates apoptosis through repression of NIK in ATL cell lines.

Tumor cells from ATL patients primarily represent the malignant characteristics. In fact, miR-31 loss is found from patient samples (Figures 1 and 3A). To demonstrate the responsibility of miR-31 for tumor cell survival, we tested whether lentivirus-mediated miR-31 expression has a killing effect against tumor cells. After establishment of lentivirus infection, the apoptotic cells were determined by flow cytometry. The results revealed that expression of miR-31 facilitated tumor cell death. Since NIK repression by shRNA lentivirus also showed a strong killing effect, NIK and NF-κB activity are suggested as crucial players for survival in ATL tumor cells (Figure 3K). Strong toxicities were not observed in normal resting lymphocytes that express low levels of NIK. Taken together, these lines of experimental evidence, including data from cell lines and primary ATL cells, definitively support two notions that (1) miR-31 acts as a tumor suppressor in T cells, and (2) NIK-regulated NF-κB has pivotal importance in cancer cell survival.

Loss of miR-31 Occurs in T Cells with Genetic and Epigenetic Abnormalities

The results described above together with previous publications indicate that regulation of miR-31 expression has profound impacts on multiple functions in human tumors as well as in normal cells. However, little is known about the regulatory mechanism of miR-31 expression. The human gene that encodes miR-31, *hsa-miR-31*, is located at 9p21.3, which is

(H–K) miR-31 attenuates signal-dependent NF-κB activation in B cells. (H and I) BJAB cells expressing miR-31 or control RNA were treated with BAFF (0.2 μg/ml) or CD40L (0.5 μg/ml) for indicated time periods. The protein levels of NIK, phospho-IKKα/β, p100/p52 (arrowheads indicate active p52), and phospho-IκBα were shown. Actin was detected as control. (J) NF-κB activity (n = 5, mean ± SD) evaluated by NF-κB-luciferase reporter assay at 24 hr after cytokine treatments. (K) NF-κB-dependent gene expressions were inhibited by miR-31 (n = 3, mean ± SD). See also Table S2 and Figure S1.

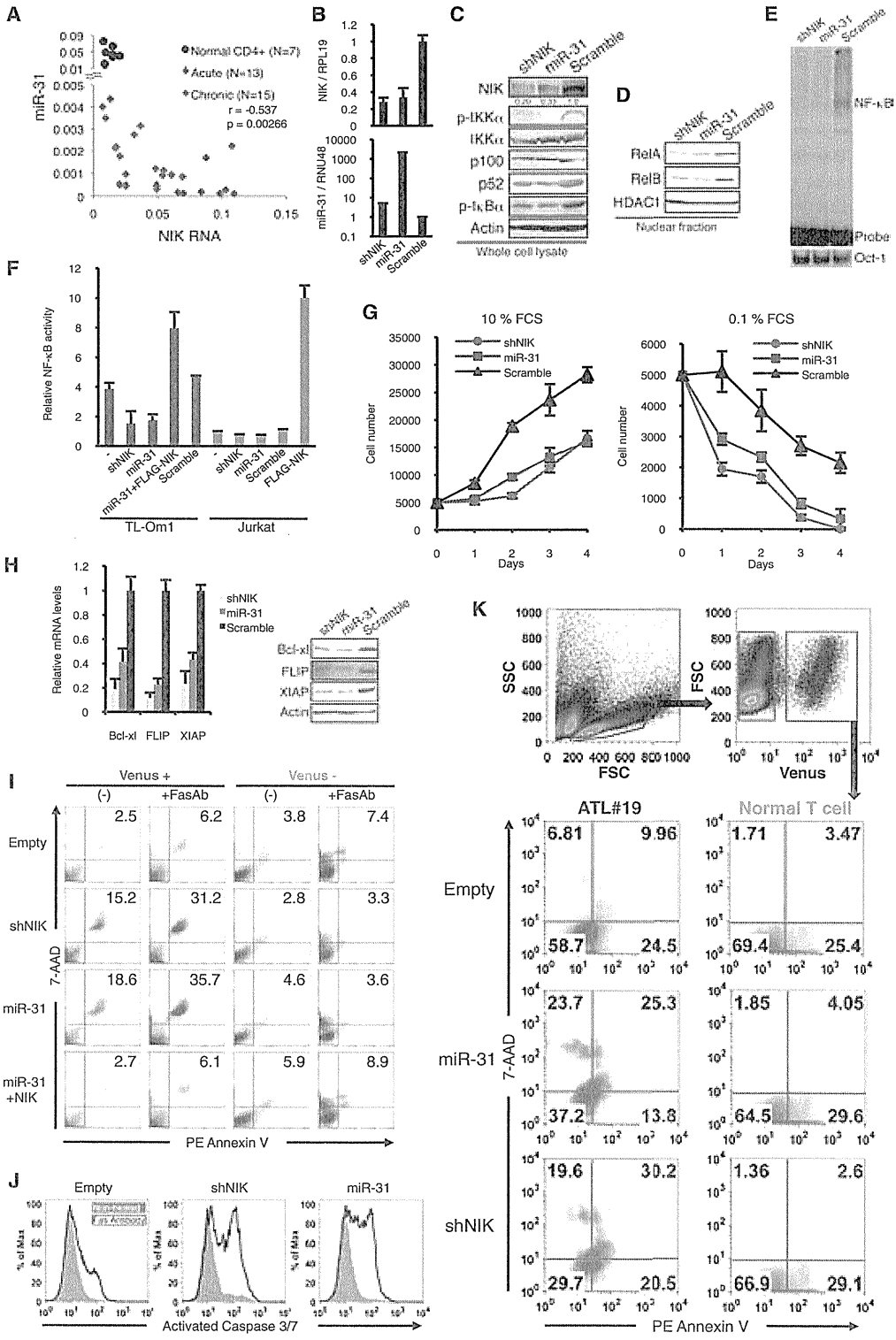

Figure 3. Loss of miR-31 Is Responsible for Constitutive NF-κB Activation, Abnormal Cell Growth, and Resistance to Apoptotic Cell Death in ATL Cells

(A) Expression levels of miR-31 and *NIK* in individual ATL patients and normal controls using data set obtained by quantitative RT-PCR. Pearson's correlation coefficient within ATL samples was described in the graph.

adjacent to clusters of the *CDKN2* and *IFNA* families, and is a well-known hotspot of genomic loss in several types of human cancers. We performed genome-wide scans of genetic lesions in 168 ATL samples and demonstrated that 21 ATL cases (12.5%) had genomic deletion of 9p21.3 containing the *hsa-miR-31* coding region (Figure 4A; Figure S3A). All of these cases also have genomic defect in *CDKN2A* region. A major proportion of ATL cases that are without genetic deletion and somatic mutation in the *hsa-miR-31* region showed remarkable loss of miR-31 expression (Figure 4B). Detailed expression profiling revealed drastic downregulation of *Pri-miR-31* transcription in the primary ATL cells (Figure 4C). There was a strong correlation between the levels of mature miR-31 and primary transcript ($r = 0.9414$, $p = 5.45 \times 10^{-8}$). *hsa-miR-31* is located in intronic region of *LOC554202* gene. However, *LOC554202* mRNA levels were very low in primary T cells and there was no significant difference between ATL and normal cells, strongly suggesting that loss of miR-31 expression is due to specific transcriptional suppression in ATL cells. Using computational analysis, we identified a putative TATA box and transcriptional start site (TSS) 2500 bp upstream of the miR-31 coding region (Figure 4D). Although no CpG islands were found in this region, we unexpectedly discovered an assembly of YY1-binding motifs upstream of the miR-31 region in human and mouse (Figure 4D; Figure S3C). YY1 is a pivotal transcription factor and a recruitor of the Polycomb repressive complex (PRC) (Simon and Kingston, 2009). Convergence of the YY1 binding sequence, especially the repressive motif (Figure S3D), seems to be evolutionarily conserved, suggesting that YY1 is important in the regulation of miR-31 transcription. We further performed chromatin immunoprecipitation (ChIP) to evaluate repressive histone hallmarks, including di- and trimethylated H3K9 (H3K9me2 and H3K9me3) and trimethylated H3K27 (H3K27me3). The results showed higher levels of methylation at H3K9 and H3K27 in a broad area containing the miR-31 coding region (Figure 4E). As shown in Figures S3E–S3G, there was an inverse correlation between the levels of miR-31 expression and repressive histone methylation. These data allowed us to hypothesize that histone methylation, especially that of Polycomb family-dependent H3K27me3, may contribute to miR-31 repression. To confirm our hypothesis, we performed a YY1 knockdown experiment using a specific shRNA (Figures 4F–4I). As expected, knockdown of YY1 led to an increase in the levels of *Pri-miR-31* and mature miR-31 (Figures 4F and 4G). Furthermore, ChIP assays showed that YY1 occupied the miR-31 region, especially in the upstream region of TSS, where there is an array of YY1 binding sites (Figures 4D and 4H). The results also demonstrated that decreased occupancy of YY1 and concomitant derecruitment of EZH2, a key component of PRC2, were induced by YY1 knockdown, indicating involvement of EZH2 in the repressive complex recruited to the miR-31 region (Figures 4H and 4I; Figure S3H). These results collectively suggest that YY1 regulates PRC2 localization and initiates miR-31 suppression. Indeed, we found significant escalation of methylated histone H3K9 and H3K27 at the miR-31 locus of peripheral blood lymphocytes of ATL patients (Figure 4J), indicating that aberrant abundance of suppressive histone methylation may be responsible for the loss of miR-31 in the primary ATL cells.

Overexpression of PRC2 Components Leads to miR-31 Repression

Given that Polycomb-mediated repressiveness affects miR-31 level, our findings imply that the amount of EZH2 is related to miR-31 expression (Figure 4I; Figures S3G and S4A). We found a significantly upregulated expression of PRC2 components, especially EZH2 and SUZ12, in the primary ATL cells (Figures 5A and 5B; Table S3). Quantitative RT-PCR revealed that miR-31 levels inversely correlated with both *EZH2* and *SUZ12*, respectively (Figure 5C). miR-101 and miR-26a, which are putative negative regulators of EZH2, seem to be associated with this relationship in ATL cells (Figures S4B–S4E). To further confirm our hypothetical mechanism linking the epigenetic machinery and miR-31 expression, we performed a "loss-of-PRC2-function" assay. Retroviral delivery of shSUZ12 and shEZH2 in the ATL cell lines resulted in a great increase in the levels of *Pri-miR-31* and its mature form (Figure 5D; Figure S4F). Knockdown of PRC2 induced histone demethylation at H3K27 in the miR-31 region, which is concomitant with the decrease in H3K9me3 levels, EZH2 occupancy, and HDAC1 recruitment (Figure 5E), suggesting that this multimeric complex leads to a completely closed chromatin architecture as a result of histone modifications in the miR-31 genomic region.

To further examine whether the proposed mechanism holds true in other human cancers, we analyzed a couple of carcinoma cell lines, including HeLa cells and nonmetastatic and metastatic breast carcinoma cell lines, MCF7 and MDA-MB-453 cells, respectively. qRT-PCR revealed that expression of *EZH2* and *SUZ12* inversely correlated with miR-31 levels (Figure S4G).

(B) miR-31 restoration by retroviral vector inhibits *NIK* RNA accumulation in TL-Om1 cells. The results of *NIK* and mature miR-31 quantifications are shown (n = 3, mean ± SD).
(C) miR-31 or shNIK expression downregulates NIK protein expression and inhibits downstream pathway of noncanonical NF-κB in TL-Om1 cells.
(D) Reduced nuclear translocation of RelA and RelB proteins in miR-31- or shNIK-expressing TL-Om1 cells.
(E) miR-31-dependent downregulation of NF-κB activity in TL-Om1 cells examined by EMSA.
(F) NF-κB-luciferase reporter assays (n = 5, mean ± SD). FLAG-NIK plasmid was transiently introduced 48 hr prior to the assay.
(G) miR-31 level is relevant to proliferation of ATL cells. Cell proliferation curve of TL-Om1 cells were evaluated in two FCS conditions (n = 3, mean ± SD).
(H) Apoptosis-related gene expression in TL-Om1 cells analyzed by qRT-PCR (n = 3, mean ± SD) and western blots.
(I) Lentivirus-mediated NIK depletion promotes basal and Fas antibody-mediated apoptosis. Venus-positive population represented lentivirus-infected cells. Apoptotic cells were determined by PE-Annexin V / 7-AAD stainings (n = 4). Representative FACS analyses are shown.
(J) miR-31 activates Caspase 3/7 determined by FACS (n = 3).
(K) miR-31 expression and NIK depletion induce tumor cell death. Primary tumor cell from ATL patient and healthy CD3+ T cells were infected with lentivirus and analyzed by FACS. The apoptotic cells were defined by sequential gating beginning with FSC-SSC to select intact lymphocytes, subgating on the Venus-positive population, and calculating the PE-Annexin V and 7-AAD profilings. Representative result is shown and summarized data are presented in Figure 6J. See also Figure S2.

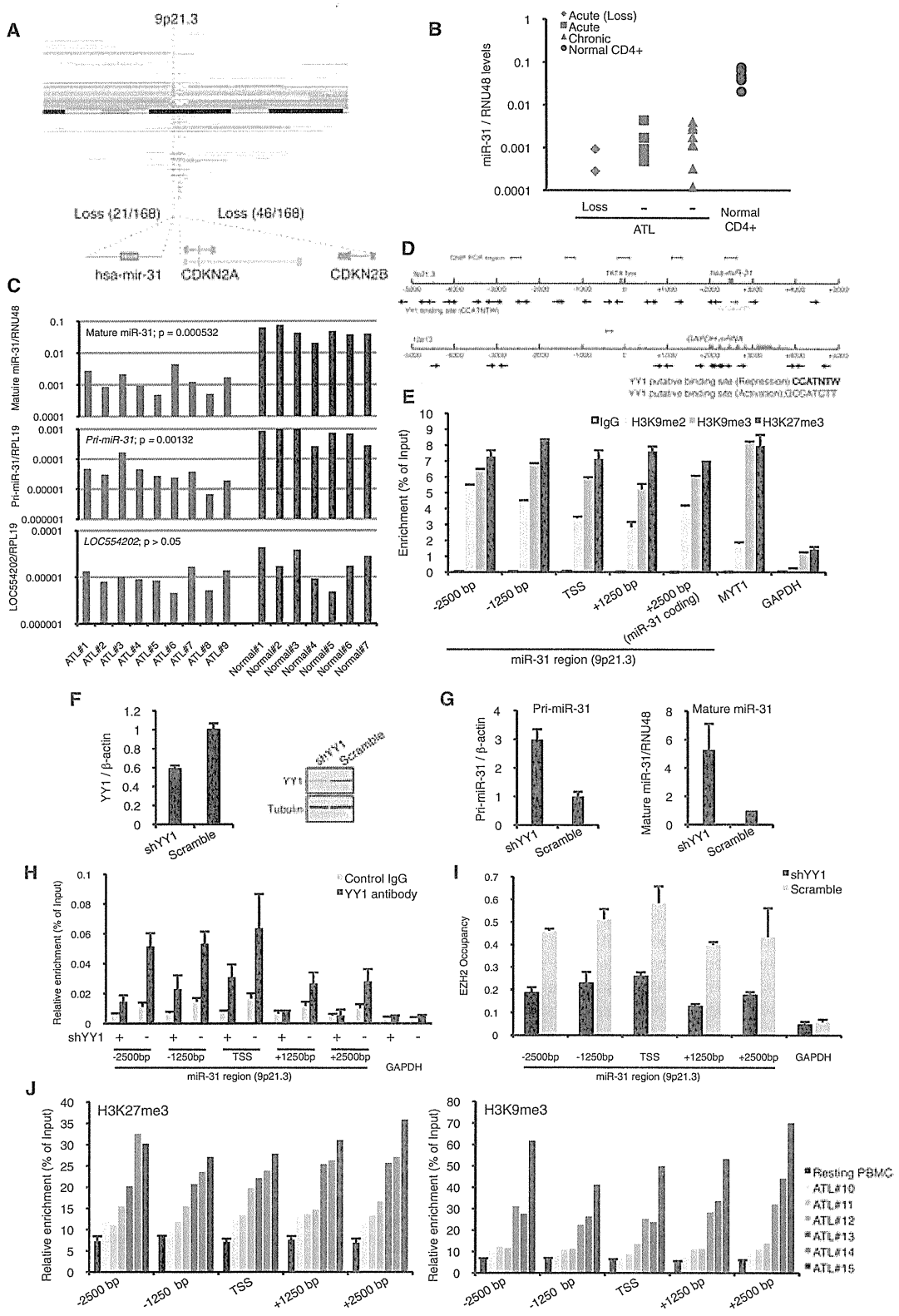
A
9p21.3
Loss (21/168)
Loss (46/168)
hsa-mir-31
CDKN2A
CDKN2B
B
Acute (Loss)
Acute
Chronic
Normal CD4+
miR-31 / RNU48 levels
Loss
ATL
Normal CD4+
C
Mature miR-31; p = 0.000532
Pri-miR-31; p = 0.00132
LOC554202; p > 0.05
Mature miR-31/RNU48
Pri-miR-31/RPL19
LOC554202/RPL19
ATL#1 ATL#2 ATL#3 ATL#4 ATL#5 ATL#6 ATL#7 ATL#8 ATL#9
Normal#1 Normal#2 Normal#3 Normal#4 Normal#5 Normal#6 Normal#7
D
YY1 putative binding site (Repressor) CCATNTW
YY1 putative binding site (Activator) GCCATCTT
E
IgG H3K9me2 H3K9me3 H3K27me3
Enrichment (% of Input)
-2500 bp
-1250 bp
TSS
+1250 bp
+2500 bp (miR-31 coding)
MYT1
GAPDH
miR-31 region (9p21.3)
F
YY1 / β-actin
shYY1
Scramble
YY1
Tubulin
G
Pri-miR-31
Pri-miR-31 / β-actin
Mature miR-31
Mature miR-31/RNU48
H
Control IgG
YY1 antibody
Relative enrichment (% of Input)
shYY1
-2500bp -1250bp TSS +1250bp +2500bp GAPDH
miR-31 region (9p21.3)
I
shYY1
Scramble
EZH2 Occupancy
-2500bp -1250bp TSS +1250bp +2500bp GAPDH
miR-31 region (9p21.3)
J
H3K27me3
H3K9me3
Relative enrichment (% of Input)
-2500 bp
-1250 bp
TSS
+1250 bp
+2500 bp
Resting PBMC
ATL#10
ATL#11
ATL#12
ATL#13
ATL#14
ATL#15

ChIP assays detected higher levels of trimethylated H3K27 and EZH2 occupancy in cells showing lower expression levels of miR-31 (Figure S4H). Furthermore, knockdown of EZH2 or SUZ12 restored miR-31 transcription in MDA-MB-453 and MCF7 cells (Figures 5F and 5G; Figure S4K, respectively), which are consistent with the results obtained with ATL cells. These results indicate a link between Polycomb-mediated epigenetic regulation and miR-31 transcription in ATL and breast cancer cell lines.

Polycomb Group Regulates NF-κB Pathway by Controlling miR-31 Expression

Based on our findings, we considered an aspect of the biological communication between epigenetic silencing and the NF-κB pathway through miR-31 regulation. The microarray data sets showed positive correlations between PRC2 components and miR-31 target gene, *NIK* expression (Figure 6A). The results also suggested that these factors tend to show higher levels in the aggressive subtype (acute type) than in the indolent subtypes (chronic and smoldering types), implying that these genes may play important roles in the clinical phenotype and prognosis of ATL. To examine this notion, we performed PRC2 knockdown in ATL cell lines. Western blots of these cells demonstrated decreased levels of NIK, p52, and phospho-IκBα (Figure 6B; Figure S5A), suggesting suppression of both canonical and noncanonical NF-κB cascade and activity (Figure 6C; Figures S5B and S5C). These results are consistent with those of miR-31 overexpression (Figures 3C–3F). Then, we tested whether exogenous manipulation of miR-31 could restore the effect of PRC2 loss. Anti-miR-31 treatment rescued impaired NF-κB activity in PRC2-disrupted cells (Figure 6D). On the other hand, overexpression of EZH2 induced NF-κB activation, which was partially canceled by the introduction of miR-31 precursor (Figure 6E; Figure S5D). These results suggest that Polycomb-mediated miR-31 suppression leads to NF-κB activation. Indeed, knockdown of the PRC2 complex led to reduced levels of cell proliferation and greater sensitivity to serum deprivation in ATL cells (Figure 6F; Figure S5E). In addition, PRC2 disruption showed a reduction in cell migration (Figure S5F).

To gain further insight into this general network, we studied the functions of miR-31 and the PRC2 complex in breast cancer cell lines. NF-κB activity was downregulated by knockdown of PRC2 components in MDA-MB-453 cells (Figure 6G; Figures S5G and S5H), although no significant differences were observed in cell proliferation (data not shown). Repression of NF-κB activity induced by knockdown of PRC2 components was partially restored by treatment with a miR-31 inhibitor, suggesting that PRC2 knockdown-mediated relief of NF-κB repression is at least a part of the result of the miR-31 induction. In addition, knockdown of PRC2 components resulted in a reduced level of receptor-initiated accumulation of NIK in B cells (Figure 6H). Our findings indicate a common molecular mechanism comprising Polycomb-mediated epigenetic regulation, miR-31 expression and the NF-κB signaling pathway.

Regulation of NF-κB by Polycomb family may in turn control the cellular apoptosis responses. We found that lentivirus-mediated EZH2 knockdown led to increased apoptotic sensitivity in TL-Om1 cells (Figure 6I). Additional expression of NIK inhibited the cell death induced by EZH2 knockdown, suggesting the reciprocal relationship between Polycomb and NF-κB cascades. By using primary tumor cells from patient, we tested the killing effect induced by miR-31, NIK knockdown, and EZH2 knockdown (Figure 6J; Figures S5I and S5J). All tested samples showed strong death response, demonstrating that survival of ATL cells was closely associated with miR-31, NIK, and EZH2, all of which show deregulated expression in ATL cells.

By qRT-PCR we finally examined the expression levels of some genes involved in the noncanonical NF-κB pathway. As shown in Figure 6K, the results clearly demonstrated higher expression levels of positive regulators such as *NIK*, *CD40,* and *LTBR*, and lower expression levels of the negative regulators such as *BIRC2/3* (cIAP1/2), which are involved in proteasomal degradation of NIK (Zarnegar et al., 2008a). These observations are in line with a previous report on Multiple Myeloma cells (Annunziata et al., 2007). In addition to these data, we obtained convincing evidence for a molecular aspect of NIK accumulation in ATL cells. Polycomb-dependent epigenetic gene silencing may be associated with miR-31 loss, followed by NF-κB activation and other signaling pathways (Figure 7).

DISCUSSION

Constitutive activation of NF-κB contributes to abnormal proliferation and inhibition of apoptotic cell death in cancer cells,

Figure 4. Genetic and Epigenetic Abnormalities Cause miR-31 Loss in ATL Cells

(A) Genomic loss of chromosome 9p21.3 in primary ATL cells. Copy number analyses revealed tumor-associated deletion of miR-31 region (21/168) and *CDKN2* region (46/168). Recurrent genetic changes are depicted by horizontal lines based on CNAG output of the SNP array analysis.

(B) miR-31 expression in various sample sets. Expression levels were evaluated by real-time PCR.

Loss, samples with genomic loss of the miR-31 region; (–) samples without genomic loss of the miR-31 region.

(C) PCR-based miR-31 quantifications in primary ATL samples. ATL samples without genetic loss in miR-31 region (n = 9, Figure S3B), and normal CD4+ T cells (n = 7) were tested. p values (ATL versus normal) are shown.

(D) YY1 binding motif cluster around transcriptional start site (TSS) of miR-31 region. Arrows represent positions of the motifs. Regions of PCR amplification for ChIP assay are shown.

(E) Repression-associated histone methylation in miR-31 region determined by ChIP assay (n = 3, mean ± SD). The results of relative enrichment against input control are presented and distance from miR-31 TSS is described. *MYT1* and *GAPDH* promoters are as positive or negative controls, respectively.

(F–I) YY1-dependent EZH2 occupancy in miR-31 locus. (F) YY1 knockdown in TL-Om1 cells. qRT-PCR (left, n = 3, mean ± SD) and western blotting (right) showed decreased YY1 level. (G) YY1 knockdown led to both primary and mature miR-31 restoration in TL-Om1 cells (n = 3, mean ± SD). (H) YY1 occupancy in miR-31 region analyzed by ChIP (n = 3, mean ± SD). YY1 occupancy in miR-31 locus was reduced by YY1 knockdown. (I) EZH2 occupancy in miR-31 region analyzed by ChIP (n = 3, mean ± SD). YY1 knockdown inhibited EZH2 recruitment in miR-31 region.

(J) Aberrant accumulation of repression-associated histone methylations widely in miR-31 region of primary ATL cells. PBMCs freshly isolated from ATL patients (n = 6) were analyzed by ChIP assay. PBMC from healthy adults were used for normal controls. See also Figure S3.

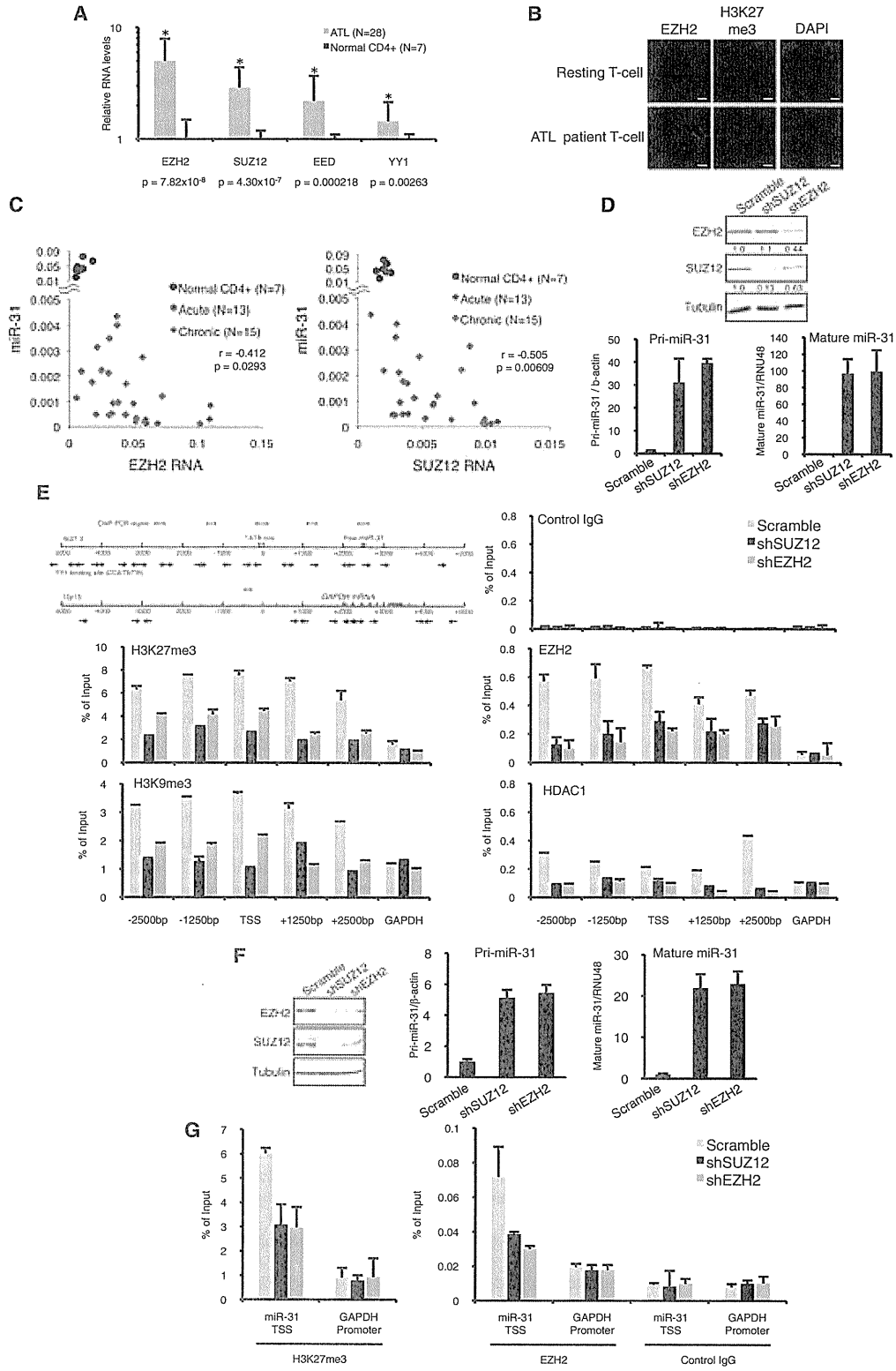
A
Relative RNA levels
ATL (N=28)
Normal CD4+ (N=7)
EZH2
SUZ12
EED
YY1
p = 7.82x10-8
p = 4.30x10-7
p = 0.000218
p = 0.00263
B
H3K27 me3
EZH2
DAPI
Resting T-cell
ATL patient T-cell
C
miR-31
Normal CD4+ (N=7)
Acute (N=13)
Chronic (N=15)
r = -0.412
p = 0.0293
EZH2 RNA
r = -0.505
p = 0.00609
SUZ12 RNA
D
Scramble
shSUZ12
shEZH2
EZH2
SUZ12
Tubulin
Pri-miR-31
Pri-miR-31 / b-actin
Mature miR-31
Mature miR-31/RNU48
E
Control IgG
Scramble
shSUZ12
shEZH2
% of Input
H3K27me3
EZH2
H3K9me3
HDAC1
-2500bp
-1250bp
TSS
+1250bp
+2500bp
GAPDH
F
Pri-miR-31
Pri-miR-31/β-actin
Mature miR-31
Mature miR-31/RNU48
G
miR-31 TSS
GAPDH Promoter
H3K27me3
EZH2
Control IgG

including ATL, diffuse large B cell lymphoma (DLBCL), Hodgkin lymphoma, breast cancer, prostate cancer and others (Prasad et al., 2010). NF-κB is also essential for various cell functions, including inflammation, innate immunity, and lymphocytic development (Hayden and Ghosh, 2008). Identification of NF-κB determinants will lead to marked progress in understanding molecular pathology.

Our global analyses demonstrated an interesting miRNA expression signature as well as an aberrant mRNA expression profile, which may be associated with leukemogenesis in the primary ATL cells (Figures 1 and 6A). We revealed downregulation of tumor-suppressive miRNA including Let-7 family, miR-125b, and miR-146b, which can contribute to aberrant tumor cell signaling. Recent studies have suggested unique expression profiles of miRNAs in ATL (Yeung et al., 2008; Bellon et al., 2009), but loss of miR-31 has not been focused. Cellular amount of miRNAs may be susceptible to various environments such as transcriptional activity, maturation processing, and also epigenetic regulation. The end results appear to be affected by methodology employed and conditions and types of samples used. Our integrated expression profiling of primary ATL cells are based on a significantly larger number of samples and fruitfully provides intriguing information that may be useful in improving the understanding of T cell biology as well as in the identification of biomarkers for diagnosis.

Pleiotropy of miR-31 was first reported by Valastyan et al. (2009). The authors elegantly demonstrated the function of miR-31 in vivo and also identified several target genes that contribute to cell migration and invasiveness. In the present study, we focused on the functional significance of miR-31 in the regulation of NF-κB signaling that contributes to tumor cell survival.

Overexpression of NIK acts as an oncogenic driver in various cancers. In the present study, NIK was identified as a miR-31 target based on several lines of evidence. First, luciferase-3′ UTR reporter assay showed that *NIK* 3′ UTR sequence has a role for negative regulation (Figure S1B). By combining a specific inhibitor and mutations in miR-31-binding site, we demonstrated that miR-31 recognizes and negatively regulates the *NIK* 3′ UTR (Figures 2A and 2D). Second, by introducing a miR-31 precursor or inhibitor, we showed that amount of miR-31 inversely correlates with levels of NIK expression and downstream signaling (Figures 2E–2K). Third, genetic evidence indicated strong base pairing and biological conservation (Bartel, 2009) (Figures S1L–S1O). Our experimental approach illustrated that mmu-miR-31 regulates mouse *Map3k14* gene. Fourth, individual assessments using gene expression data clearly revealed an inverse correlation between the expression levels of miR-31 and *NIK* (Figure 3A). Collectively, we provide definitive evidence for the notion that miR-31 negatively regulates NIK expression and activity.

It is well known that the NIK level directly regulates NF-κB activity in various cell types (Thu and Richmond, 2010). We experimentally showed that miR-31 regulates noncanonical NF-κB activation stimulated by BAFF and CD40L, both of which are major B cell activating cytokines. Since signals from receptors are essential for the development and activity of B cells, the negative role of miR-31 in cytokines-induced NIK accumulation appears to be widely important in the noncanonical regulation of NF-κB in B cells and other cell types (Figures 2H–2K). Again, our findings revealed the role of NIK in the regulation of canonical NF-κB pathway. Strict regulation of NIK appears to be closely associated with the fate of lymphocytes.

The level of miR-31 was drastically suppressed in all tested primary ATL cells, and its magnitude is greater than that which has been reported in other cancers. Our results demonstrated a profound downregulation of miR-31 (fold change, 0.00403; Figure 1B) in all ATL cases, suggesting that miR-31 loss is a prerequisite for ATL development. Restoration of miR-31-repressed NF-κB activity in ATL cells, resulting in impairment of the proliferative index and apoptosis resistance (Figure 3). Furthermore, our results demonstrate that inhibition of NF-κB promotes tumor cell death in cell lines and also primary tumor cells from ATL patients (Figures 3 and 6), which are consistent with our previous observation (Watanabe et al., 2005). Since it is highly possible that miR-31 and relevant factors are pivotal in cancers, their expressions would have a great importance in view of biomarkers for the aberrant signaling and clinical outcomes.

By studying clinical samples and in vitro and ex vivo models, we obtained several biologically interesting results. First, we identified the Polycomb protein complex as a strong suppressor of miR-31. Generally, the Polycomb group constitutes a multimeric complex that negatively controls a large number of genes involved in cellular development, reproduction, and stemness (Sparmann and van Lohuizen et al., 2006). However, the key molecules involved in cancer development, progression, and prognosis are not yet fully understood. In breast and prostate cancers, oncogenic functions of EZH2 and NF-κB activation were reported independently (Kleer et al., 2003; Varambally et al., 2002; Suh and Rabson, 2004). Interestingly, these tumors show low miR-31 levels (Valastyan et al., 2009; Schaefer et al., 2010). Recently, Min et al. (2010) reported that EZH2 activates NF-κB by silencing the DAB2IP gene in prostate cancer cells.

Figure 5. Amount of PRC2 Components Epigenetically Links to miR-31 Expression in T Cells and Epithelial Cells

(A) Overexpression of PRC2 components in primary ATL cells measured by qRT-PCR (ATL, n = 28; normal, n = 7; mean ± SD). These results were supported by the data of gene expression microarray (Table S3).

(B) Escalation of EZH2 protein and trimethylated H3K27 levels in primary ATL cells illustrated by immunocytostaining (n = 4, a representative result is shown). Resting T cells were as normal control. Scale bars = 20 μm.

(C) Statistical correlation among the levels of miR-31, *EZH2*, and *SUZ12* in individual ATL samples. Correlation coefficients within ATL samples are shown in the graphs.

(D and E) Loss of PCR2 function causes chromatin rearrangement and miR-31 upregulation. (D) TL-Om1 cells expressing shSUZ12, shEZH2, and scrambled RNA were established by retroviral vector. The levels of EZH2, SUZ12, *Pri-miR-31*, and mature miR-31 were measured by western blotting and qRT-PCR (n = 3, mean ± SD). (E) Results of ChIP assays with indicated antibodies (n = 3, mean ± SD). Amounts of immunoprecipitated DNA were analyzed by region-specific PCR. *GAPDH* promoter served as a region control.

(F and G) Knockdown of Polycomb family proteins in MDA-MB-453 cells. (F) EZH2 and SUZ12 are shown by western blot. miR-31 level was examined by qRT-PCR (n = 3, mean ± SD). (G) Histone methylation and EZH2 occupancy evaluated by ChIP assay (n = 3, mean ± SD). See also Table S3 and Figure S4.

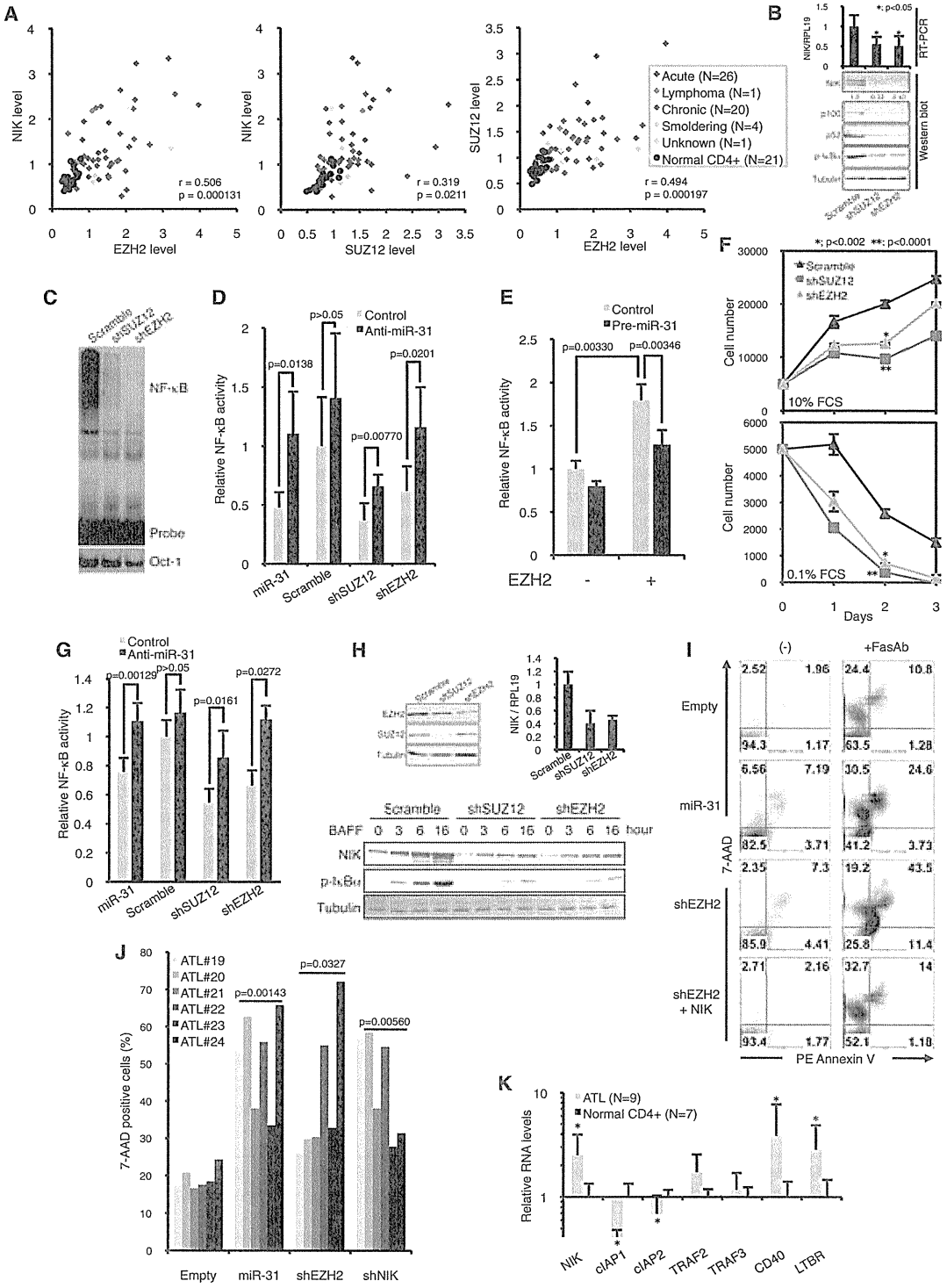

Figure 6. Epigenetic Change Driven by Polycomb Group Mediates NF-κB Signaling through miR-31 Regulation

(A) Reciprocal relationship of mRNA expression between *NIK* and Polycomb group in primary samples. Pearson's correlation coefficients among ATL samples are shown.

(B) PRC2 knockdown negatively affects NF-κB signaling in TL-Om1 cells. After establishment of PRC2 knockdown, the levels of *NIK* RNA (n = 4, mean ± SD) and proteins of NIK, p52/p100, and phospho-IκBα were examined.

(C) Downregulation of NF-κB activity in PRC2-disrupted cells detected by EMSA.

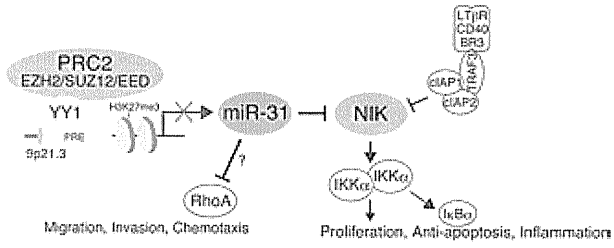

Figure 7. Proposed Model for ATL and Other Tumor Cells
Polycomb repressive factors are linked to NIK-dependent NF-κB activation via miR-31 regulation.

In the present study, we found that the Polycomb group regulates miR-31 expression and that elevated expression of EZH2 leads to NF-κB activation via NIK-miR-31 regulation in ATL and breast cancer cells (Figure 6). We also showed that restoration of miR-31 partially impaired Polycomb-mediated NF-κB operation (Figures 6D, 6E, and 6G), suggesting that miR-31 is involved in this relationship. Furthermore, a connection between NIK and PRC2 was observed in B cells (Figure 6H). Polycomb group proteins are essential in lymphocyte development and activation (Su et al., 2003, 2005). Further, given the NF-κB is a pivotal transcription regulator in normal and oncogenic functions, practical participations of epigenetic regulators and miR-31 in NF-κB signaling will increase our understanding of the molecular mechanisms of T cell functions. For generalization of the molecular axis in other cancers and normal cells, further study will be needed.

Second, YY1 is a recruiter of PRC2 to the miR-31 region. In humans, the Polycomb response element (PRE) has not been precisely identified. A good candidate for a mammalian recruiter of PRC2 is YY1, the homolog of *D. melanogaster* PHO (Simon and Kingston, 2009). We found an assembly of the YY1 binding motif in the miR-31 locus and demonstrated that YY1 knockdown dislodged EZH2 in this region (Figure 4I), which supports previous findings (Caretti et al., 2004). The detailed mechanism by which YY1 mediates recruitment of the Polycomb family may be important in the context of epigenetic regulation of orchestrated gene expression and T cell functions.

Third, Polycomb family proteins can control miRNA expression in an epigenetic fashion. The amount of PRC2 factors strongly influenced the degree of suppression of miR-31 expression (Figure 5). We speculate that, in addition to controlling the transcription, the Polycomb group can modulate translation via miRNA regulation. Furthermore, miR-101 and miR-26a are known to regulate EZH2 expression (Sander et al., 2008; Varambally et al., 2008), which is supported by our observation (Figure S4C). This signaling circuit will permit multiple gene regulation. Whereas genetic loss at the miR-31 locus is observed in some cases of ATL (Figure 4A), no genetic deletion in the miR-101-1 or miR-101-2 region was detected in ATL, which is not consistent with a previous finding in prostate cancer. Our results also suggested putative association between Let-7 family and EZH2 (Figure S4). Aberrant downregulations of these miRNAs in the primary ATL cells will be the next important questions to be addressed in efforts to improve understanding of the oncogenic signaling network.

By collaborative profiling of miRNA and mRNA expression, we identified a notable relationship between ATL subtypes and a gene cluster that contains miR-31, NIK, EZH2, and SUZ12. This finding suggests that an aberrant gene expression pattern correlates with the malignant phenotype, and this provides important clues about clinical manifestations and may help identify therapeutic targets against ATL cells (Figure 6A). Although HDAC inhibitors did not show effective responses (Figures S4I and S4J), emerging epigenetic drug such an EZH2 inhibitor (Fiskus et al., 2009) may pave a pathway leading to cures for various malignancies that involve constitutive activation of NF-κB.

In summary, we show that genetic and epigenetic loss of miR-31 is responsible for oncogenic NF-κB activation and malignant phenotypes in ATL. This provides evidence for the idea that miR-31 is an important tumor suppressor. An emerging pathway involving an epigenetic process, miR-31, and NF-κB will provide a conceptual advance in epigenetic reprogramming, inflammatory signaling, and oncogenic addiction.

EXPERIMENTAL PROCEDURES

Cell Lines and Primary ATL Cells

The primary peripheral blood mononuclear cells (PBMCs) from ATL patients and healthy volunteers used in the present work were a part of those collected with an informed consent as a collaborative project of the Joint Study on Prognostic Factors of ATL Development (JSPFAD). The project was approved by the Institute of Medical Sciences, the University of Tokyo (IMSUT) Human Genome Research Ethics Committee. Additional ATL clinical samples for copy number analysis were provided by Drs. Y. Yamada, Nagasaki University,

(D) NF-κB activity evaluated by reporter assays in the presence or absence of miR-31 inhibitor (n = 5, mean ± SD). Anti-miR-31 treatment partially rescued the NF-κB activity in PRC2 knockdowned TL-Om1 cells.
(E) Overexpressed EZH2 activates NF-κB via miR-31. Jurkat cells were transfected with an EZH2 plasmid together with miR-31 precursor or control RNA (n = 5, mean ± SD).
(F) PRC2 dysfunction changes TL-Om1 cell proliferation and response to serum starvation. Under conditions of 10% or 0.1% of FCS, cell growth curves were examined (n = 3, mean ± SD). PRC2 downregulation decreased cell growth with statistical significance.
(G) NF-κB activity in PRC2-knockdowned MDA-MB-453 cells in the presence or absence of miR-31 inhibitor were examined (n = 5, mean ± SD).
(H) PRC2 disruption inhibits BAFF-dependent NIK accumulation and IκBα phosphorylation in BJAB cells.
(I) Apoptotic cell death induced by lentivirus-mediated EZH2 knockdown in TL-Om1. Venus-positive populations were analyzed by Annexin V/7-AAD stainings (n = 3) and representative of FACS data are shown.
(J) Summary of primary tumor cell death. Lentivirus-based miR-31 expression, NIK knockdown, and EZH2 knockdown showed killing effects in six primary ATL samples. Statistical significances are shown in the graph. Results of FACS and qRT-PCR are shown in Figures S5I and S5J.
(K) Expression levels of genes involved in noncanonical NF-κB pathway in primary ATL cells (ATL, n = 9; normal, n = 7; mean ± SD). Relative expression levels were tested by qRT-PCR (*$p < 0.05$). See also Figure S5.

and K. Ohshima, Kurume University, where the projects were approved by the Research Ethics Committees of Nagasaki University and Kurume University, respectively. PBMC were isolated by Ficoll separation. ATL cells, primary lymphocytes, and all T cell lines were maintained in RPMI1640 supplemented with 10% of FCS and antibiotics. Clinical information of ATL samples is provided in Table S1.

Expression Analyses

Clinical samples for microarrays were collected by a collaborative study group, JSPFAD (Iwanaga et al., 2010). Gene expression microarray was used 4x44K Whole Human Genome Oligo Microarray (Agilent Technologies) and miRNA microarray was used Human miRNA microarray kit v2 (Agilent Technologies), respectively. Quantitative RT-PCR was performed with SYBRGreen (TAKARA). Mature miRNA assays were purchased from Applied Biosystems.

Copy Number Analyses

Genomic DNA from ATL patients was provided from the material bank of JSPFAD, Nagasaki University, and Kurume University, and was analyzed by Affymetrix GeneChip Human Mapping 250K Nsp Array (Affymetrix). Obtained data were analyzed by CNAG/AsCNAR program (Chen et al., 2008).

Oligonucleotides, Plasmids, and Retrovirus Vectors

All RT-PCR primers and oligonucleotides are described in Supplemental Experimental Procedures. miRNA precursor and inhibitor were from Applied Biosystems. Transfection of small RNA and other plasmid DNA were performed by Lipofectamine2000 (Invitrogen). For miRNA or shRNA expression, retroviral vectors (pSINsi-U6, TAKARA) were used.

3′ UTR-Conjugated miR-31 Reporter Assay

HeLa cells were cotransfected with 3′ UTR-inserted pMIR-REPORT firefly plasmid (Ambion), RSV-Renilla luciferase plasmid, and miRNA inhibitor. The cells were collected at 24 hr posttransfection, and Dual-luciferase reporter assay was performed (Promega).

Analysis of NF-κB Pathway

NF-κB activity was evaluated by EMSA and reporter assays as previously described (Horie et al., 2004). Antibodies for western blots are described in supplemental information. Cell proliferative assay was performed by Cell Counting Kit-8 (Dojindo).

Lentivirus Vectors and Apoptosis Analysis

A lentivirus vector (CS-H1-EVBsd) was provided from RIKEN, BRC, Japan. Lentivirus solution was produced by cotransfection with packaging plasmid (pCAG-HIVgp) and VSV-G- and Rev-expressing plasmid (pCMV-VSV-G-RSV-Rev) into 293FT cells. After infection of lentivirus, the apoptotic cell was evaluated by PE Annexin V / 7-AAD staining (BD PharMingen) and analyzed by FACS Calibur (Becton, Dickinson). Collected data were analyzed by FlowJo software (Tree Star).

ChIP Assay

ChIP assay was previously described (Yamagishi et al., 2009). Briefly, cells were crosslinked with 1% of formaldehyde, sonicated, and subjected to chromatin-conjugated IP using specific antibodies. Precipitated DNA was purified and analyzed by real-time PCR with specific primers (see Supplemental Experimental Procedures).

Computational Prediction

To identify miR-31 target genes, we integrated the output results of multiple prediction programs; TargetScan, PicTar, miRanda, and PITA. RNAhybrid was for secondary structure of miRNA-3′ UTR hybrid. TSSG program was for TATA box and TSS predictions. DNA methylation site was predicted by CpG island Searcher.

Statistical Analyses

Data were analyzed as follows: (1) Welch's t test for Gene Expression Microarray (p value cutoff at 10^{-6}) and miRNA Microarray (p value cutoff at 10^{-5}); (2) Pearson's correlation for two-dimensional hierarchical clustering analysis and individual assessment of microarray data sets; (3) two-tailed paired Student's t test with $p < 0.05$ considered statistically significant for in vitro cell lines and primary cells experiments, including luciferase assay, RT-PCR, ChIP assay, cell growth assay, and migration assay. Data are presented as mean ± SD.

ACCESSION NUMBERS

Coordinates have been deposited in Gene Expression Omnibus database with accession numbers, GSE31629 (miRNA microarray), GSE33615 (gene expression microarray), and GSE33602 (copy number analyses).

SUPPLEMENTAL INFORMATION

Supplemental Information includes three tables, five figures, and Supplemental Experimental Procedures and can be found with this article online at doi:10.1016/j.ccr.2011.12.015.

ACKNOWLEDGMENTS

We thank Dr. M. Iwanaga, Mr. M. Nakashima, and Ms. T. Akashi for support and maintenance of JSPFAD. We thank Drs. H. Miyoshi and A. Miyawaki for providing the Venus-encoding lentivirus vectors. We also thank Dr. R. Horie for experimental advices, and Drs. T. Kanno and T. Ishida for providing the MDA-MB-453. Grant support: Grants-in-Aid for Scientific Research from Ministry of Education, Culture, Sports, Science, and Technology of Japan to T.W. (No. 23390250) and by Grants-in-Aid from the Ministry of Health, Labour and Welfare to T.W. (H21-G-002 and H22-AIDS-I-002).

Received: November 3, 2010
Revised: August 12, 2011
Accepted: December 19, 2011
Published: January 17, 2012

REFERENCES

Annunziata, C.M., Davis, R.E., Demchenko, Y., Bellamy, W., Gabrea, A., Zhan, F., Lenz, G., Hanamura, I., Wright, G., Xiao, W., et al. (2007). Frequent engagement of the classical and alternative NF-kappaB pathways by diverse genetic abnormalities in multiple myeloma. Cancer Cell *12*, 115–130.

Bartel, D.P. (2009). MicroRNAs: target recognition and regulatory functions. Cell *136*, 215–233.

Bellon, M., Lepelletier, Y., Hermine, O., and Nicot, C. (2009). Deregulation of microRNA involved in hematopoiesis and the immune response in HTLV-I adult T-cell leukemia. Blood *113*, 4914–4917.

Caretti, G., Di Padova, M., Micales, B., Lyons, G.E., and Sartorelli, V. (2004). The Polycomb Ezh2 methyltransferase regulates muscle gene expression and skeletal muscle differentiation. Genes Dev. *18*, 2627–2638.

Chen, Y., Takita, J., Choi, Y.L., Kato, M., Ohira, M., Sanada, M., Wang, L., Soda, M., Kikuchi, A., Igarashi, T., et al. (2008). Oncogenic mutations of ALK kinase in neuroblastoma. Nature *455*, 971–974.

Davis, B.N., Hilyard, A.C., Lagna, G., and Hata, A. (2008). SMAD proteins control DROSHA-mediated microRNA maturation. Nature *454*, 56–61.

Fiskus, W., Wang, Y., Sreekumar, A., Buckley, K.M., Shi, H., Jillella, A., Ustun, C., Rao, R., Fernandez, P., Chen, J., et al. (2009). Combined epigenetic therapy with the histone methyltransferase EZH2 inhibitor 3-deazaneplanocin A and the histone deacetylase inhibitor panobinostat against human AML cells. Blood *114*, 2733–2743.

Hayden, M.S., and Ghosh, S. (2008). Shared principles in NF-kappaB signaling. Cell *132*, 344–362.

Hironaka, N., Mochida, K., Mori, N., Maeda, M., Yamamoto, N., and Yamaoka, S. (2004). Tax-independent constitutive IkappaB kinase activation in adult T-cell leukemia cells. Neoplasia *6*, 266–278.

Horie, R., Watanabe, M., Ishida, T., Koiwa, T., Aizawa, S., Itoh, K., Higashihara, M., Kadin, M.E., and Watanabe, T. (2004). The NPM-ALK oncoprotein

abrogates CD30 signaling and constitutive NF-kappaB activation in anaplastic large cell lymphoma. Cancer Cell *5*, 353–364.

Iwanaga, M., Watanabe, T., Utsunomiya, A., Okayama, A., Uchimaru, K., Koh, K.R., Ogata, M., Kikuchi, H., Sagara, Y., Uozumi, K., et al; Joint Study on Predisposing Factors of ATL Development investigators. (2010). Human T-cell leukemia virus type I (HTLV-1) proviral load and disease progression in asymptomatic HTLV-1 carriers: a nationwide prospective study in Japan. Blood *116*, 1211–1219.

Kleer, C.G., Cao, Q., Varambally, S., Shen, R., Ota, I., Tomlins, S.A., Ghosh, D., Sewalt, R.G., Otte, A.P., Hayes, D.F., et al. (2003). EZH2 is a marker of aggressive breast cancer and promotes neoplastic transformation of breast epithelial cells. Proc. Natl. Acad. Sci. USA *100*, 11606–11611.

Liao, G., Zhang, M., Harhaj, E.W., and Sun, S.C. (2004). Regulation of the NF-kappaB-inducing kinase by tumor necrosis factor receptor-associated factor 3-induced degradation. J. Biol. Chem. *279*, 26243–26250.

Malinin, N.L., Boldin, M.P., Kovalenko, A.V., and Wallach, D. (1997). MAP3K-related kinase involved in NF-kappaB induction by TNF, CD95 and IL-1. Nature *385*, 540–544.

Min, J., Zaslavsky, A., Fedele, G., McLaughlin, S.K., Reczek, E.E., De Raedt, T., Guney, I., Strochlic, D.E., Macconaill, L.E., Beroukhim, R., et al. (2010). An oncogene-tumor suppressor cascade drives metastatic prostate cancer by coordinately activating Ras and nuclear factor-kappaB. Nat. Med. *16*, 286–294.

Prasad, S., Ravindran, J., and Aggarwal, B.B. (2010). NF-kappaB and cancer: how intimate is this relationship. Mol. Cell. Biochem. *336*, 25–37.

Ramakrishnan, P., Wang, W., and Wallach, D. (2004). Receptor-specific signaling for both the alternative and the canonical NF-kappaB activation pathways by NF-kappaB-inducing kinase. Immunity *21*, 477–489.

Saitoh, Y., Yamamoto, N., Dewan, M.Z., Sugimoto, H., Martinez Bruyn, V.J., Iwasaki, Y., Matsubara, K., Qi, X., Saitoh, T., Imoto, I., et al. (2008). Overexpressed NF-kappaB-inducing kinase contributes to the tumorigenesis of adult T-cell leukemia and Hodgkin Reed-Sternberg cells. Blood *111*, 5118–5129.

Sander, S., Bullinger, L., Klapproth, K., Fiedler, K., Kestler, H.A., Barth, T.F., Möller, P., Stilgenbauer, S., Pollack, J.R., and Wirth, T. (2008). MYC stimulates EZH2 expression by repression of its negative regulator miR-26a. Blood *112*, 4202–4212.

Schaefer, A., Jung, M., Mollenkopf, H.J., Wagner, I., Stephan, C., Jentzmik, F., Miller, K., Lein, M., Kristiansen, G., and Jung, K. (2010). Diagnostic and prognostic implications of microRNA profiling in prostate carcinoma. Int. J. Cancer *126*, 1166–1176.

Simon, J.A., and Kingston, R.E. (2009). Mechanisms of polycomb gene silencing: knowns and unknowns. Nat. Rev. Mol. Cell Biol. *10*, 697–708.

Sparmann, A., and van Lohuizen, M. (2006). Polycomb silencers control cell fate, development and cancer. Nat. Rev. Cancer *6*, 846–856.

Su, I.H., Basavaraj, A., Krutchinsky, A.N., Hobert, O., Ullrich, A., Chait, B.T., and Tarakhovsky, A. (2003). Ezh2 controls B cell development through histone H3 methylation and Igh rearrangement. Nat. Immunol. *4*, 124–131.

Su, I.H., Dobenecker, M.W., Dickinson, E., Oser, M., Basavaraj, A., Marqueron, R., Viale, A., Reinberg, D., Wülfing, C., and Tarakhovsky, A. (2005). Polycomb group protein ezh2 controls actin polymerization and cell signaling. Cell *121*, 425–436.

Suh, J., and Rabson, A.B. (2004). NF-kappaB activation in human prostate cancer: important mediator or epiphenomenon? J. Cell. Biochem. *91*, 100–117.

Thu, Y.M., and Richmond, A. (2010). NF-κB inducing kinase: a key regulator in the immune system and in cancer. Cytokine Growth Factor Rev. *21*, 213–226.

Trabucchi, M., Briata, P., Garcia-Mayoral, M., Haase, A.D., Filipowicz, W., Ramos, A., Gherzi, R., and Rosenfeld, M.G. (2009). The RNA-binding protein KSRP promotes the biogenesis of a subset of microRNAs. Nature *459*, 1010–1014.

Valastyan, S., Reinhardt, F., Benaich, N., Calogrias, D., Szász, A.M., Wang, Z.C., Brock, J.E., Richardson, A.L., and Weinberg, R.A. (2009). A pleiotropically acting microRNA, miR-31, inhibits breast cancer metastasis. Cell *137*, 1032–1046.

Varambally, S., Dhanasekaran, S.M., Zhou, M., Barrette, T.R., Kumar-Sinha, C., Sanda, M.G., Ghosh, D., Pienta, K.J., Sewalt, R.G., Otte, A.P., et al. (2002). The polycomb group protein EZH2 is involved in progression of prostate cancer. Nature *419*, 624–629.

Varambally, S., Cao, Q., Mani, R.S., Shankar, S., Wang, X., Ateeq, B., Laxman, B., Cao, X., Jing, X., Ramnarayanan, K., et al. (2008). Genomic loss of microRNA-101 leads to overexpression of histone methyltransferase EZH2 in cancer. Science *322*, 1695–1699.

Ventura, A., and Jacks, T. (2009). MicroRNAs and cancer: short RNAs go a long way. Cell *136*, 586–591.

Watanabe, M., Ohsugi, T., Shoda, M., Ishida, T., Aizawa, S., Maruyama-Nagai, M., Utsunomiya, A., Koga, S., Yamada, Y., Kamihira, S., et al. (2005). Dual targeting of transformed and untransformed HTLV-1-infected T cells by DHMEQ, a potent and selective inhibitor of NF-kappaB, as a strategy for chemoprevention and therapy of adult T-cell leukemia. Blood *106*, 2462–2471.

Yamagishi, M., Ishida, T., Miyake, A., Cooper, D.A., Kelleher, A.D., Suzuki, K., and Watanabe, T. (2009). Retroviral delivery of promoter-targeted shRNA induces long-term silencing of HIV-1 transcription. Microbes Infect. *11*, 500–508.

Yamaguchi, K., and Watanabe, T. (2002). Human T lymphotropic virus type-I and adult T-cell leukemia in Japan. Int. J. Hematol. *76* (*Suppl 2*), 240–245.

Yeung, M.L., Yasunaga, J., Bennasser, Y., Dusetti, N., Harris, D., Ahmad, N., Matsuoka, M., and Jeang, K.T. (2008). Roles for microRNAs, miR-93 and miR-130b, and tumor protein 53-induced nuclear protein 1 tumor suppressor in cell growth dysregulation by human T-cell lymphotrophic virus 1. Cancer Res. *68*, 8976–8985.

Zarnegar, B.J., Wang, Y., Mahoney, D.J., Dempsey, P.W., Cheung, H.H., He, J., Shiba, T., Yang, X., Yeh, W.C., Mak, T.W., et al. (2008a). Noncanonical NF-kappaB activation requires coordinated assembly of a regulatory complex of the adaptors cIAP1, cIAP2, TRAF2 and TRAF3 and the kinase NIK. Nat. Immunol. *9*, 1371–1378.

Zarnegar, B.J., Yamazaki, S., He, J.Q., and Cheng, G. (2008b). Control of canonical NF-kappaB activation through the NIK-IKK complex pathway. Proc. Natl. Acad. Sci. USA *105*, 3503–3508.

Clonal evolution of adult T-cell leukemia/lymphoma takes place in the lymph nodes

Akira Umino,[1,2] Masao Nakagawa,[1] Atae Utsunomiya,[3] Kunihiro Tsukasaki,[4] Naoya Taira,[5] Naoyuki Katayama,[2] and Masao Seto[1,6]

[1]Division of Molecular Medicine, Aichi Cancer Center Research Institute, Nagoya, Japan; [2]Hematology and Oncology, Mie University Graduate School of Medicine, Tsu, Japan; [3]Department of Hematology, Imamura Bun-in Hospital, Kamoikeshinmachi, Kagoshima, Japan; [4]Department of Hematology and Molecular Medicine Unit, Atomic Bomb Disease Institute, Nagasaki University Graduate School of Biomedical Sciences, Nagasaki, Japan; [5]Deptment of Internal Medicine, Heartlife Hospital, Okinawa, Japan; and [6]Department of Cancer Genetics, Nagoya University Graduate School of Medicine, Chikusa-ku, Nagoya, Japan

Adult T-cell leukemia/lymphoma (ATLL) is the neoplasm caused by human T-cell leukemia virus type 1 (HTLV-1). We performed oligo-array comparative genomic hybridization (CGH) against paired samples comprising peripheral blood (PB) and lymph node (LN) samples from 13 patients with acute ATLL. We found that the genome profiles of the PB frequently differed from those of the LN samples. The results showed that 9 of 13 cases investigated had a log2 ratio imbalance among chromosomes, and that chromosome imbalances were more frequent in LN samples. Detailed analysis revealed that the imbalances were likely caused by the presence of multiple subclones in the LN samples. Five of 13 cases showed homozygous loss regions in PB samples, which were not found in the LN samples, indicating that tumors in the PB were derived from LN subclones in most cases. Southern blot analysis of TCRγ showed that these multiple subclones originated from a common clone. We concluded that in many ATLL cases, multiple subclones in the LNs originate from a common clone, and that a selected subclone among the LN subclones appears in the PB. (*Blood*. 2011;117(20):5473-5478)

Introduction

Adult T-cell leukemia/lymphoma (ATLL) is the neoplasm caused by human T-cell leukemia virus type 1 (HTLV-1). The disease is associated with poor prognosis due to drug resistance, the occurrence of opportunistic infections, a large tumor burden with multi-organ failure, and hypercalcemia. Shimoyama et al[1] classified ATLL into 4 subtypes: smoldering, chronic, lymphoma, and acute. It is also known that HTLV-1 infection alone does not facilitate the progress of infected $CD4^+$ T cells to fully malignant ATLL cells. Therefore, the search for genes involved in ATLL development and for the specific genes involved in each ATLL type has been actively pursued, albeit with limited success. ATLL-specific chromosomal abnormalities have yet to be found; however, a frequent abnormality found in ATLL is 14q11, which has also been found in other types of T-cell malignancies.[2,3] HTLV-1 provirus integration sites have also been extensively sought, and the sites identified were found to be randomly located. Investigations relying on G-band and fluorescence in situ hybridization analyses have not been fruitful in providing a detailed delineation of the genomic aberrations involved.[4] The use of high-resolution, array-based comparative genomic hybridization (CGH) for comprehensive chromosome analysis should prove useful in the search for genomic aberrations. We showed previously that acute and lymphoma ATLL types possess distinct genomic profiles, as determined by bacterial artificial chromosome array CGH.[5] It should be noted, however, that when lymphoma-type ATLL progresses to manifest more than 2% flower cells in the peripheral blood (PB), it is then classified as the acute type. We set out to analyze the genomic aberrations of acute-type ATLL with paired PB and lymph node (LN) samples in more detail by oligo-array CGH.

An important factor in the diagnosis of ATLL is the identification of monoclonal integration of HTLV-1. It has been reported that the same HTLV-1–infected clone was detected over several years in a chronic-type ATLL patient.[6,7] These types of HTLV-1–infected $CD4^+$ T lymphocytes are believed to accumulate various changes during an extensive latency period of over 50 years.[8] Alterations in genomic copy number represent one example of the type of accumulated genomic changes that can occur. In the present study, we performed high-resolution oligo-array CGH (Agilent Technologies) using a 44 000-probe set against paired samples obtained from the PB and LNs of 13 patients with acute-type ATLL.

Methods

ATLL patients and cell lines

We conducted a survey of genomic profiles by examination of PB and LN samples taken from 13 patients with acute-type ATLL. Paired samples were collected from each patient within 14 days of diagnosis. The PB and LN samples, together with clinical data, were obtained from 13 patients under a protocol approved by the institutional review board of the Aichi Cancer Center. Informed consent was provided according to the Declaration of Helsinki. Patients were diagnosed from those hospitalized between 1988 and 2010 at Imamura-Bunin Hospital and Nagasaki University School of Medicine. The diagnosis of ATLL was based on clinical features, hematologic characteristics, immunophenotype, and the presence of serum antibodies to ATLL-associated antigens. The median age of the patients was

Submitted December 26, 2010; accepted March 11, 2011. Prepublished online as *Blood* First Edition paper, March 29, 2011; DOI 10.1182/blood-2010-12-327791.

The online version of this article contains a data supplement.

The publication costs of this article were defrayed in part by page charge payment. Therefore, and solely to indicate this fact, this article is hereby marked "advertisement" in accordance with 18 USC section 1734.